

Spots structure and stratification of helium and silicon in the atmosphere of He-weak star HD 21699.

A.V.Shavrina¹, Yu.V. Glagolevskij², J. Silvester^{3,4},
G.A. Chuntov², V.R. Khalack⁵, Ya.V. Pavlenko¹

¹Main Astronomical Observatory of National Academy of Sciences of Ukraine, 27 Akademika Zabolotnoho St., 03680 Kyiv, Ukraine

²Special Astrophysical Observatory of Russian Academy of Sciences, Nizhnij Arkhiz, Zelenchukskiy region, Karachai-Cherkessian Republic, Russia 369

³Department of Physics, Engineering Physics & Astronomy, Queen's University, Kingston, Ontario, Canada, K7L 3N6

⁴Department of Physics, Royal Military College of Canada, P.O. Box 17000, Station 'Forces', Kingston, Ontario, Canada, K7K 7B4

⁵Département de Physique et d'Astronomie, Université de Moncton, Moncton, N.-B., Canada E1A 3E9

ABSTRACT

The magnetic star HD 21699 possesses a unique magnetic field structure where the magnetic dipole is displaced from the centre by 0.4 ± 0.1 of the stellar radius (perpendicularly to the magnetic axis), as a result, the magnetic poles are situated close to one another on the stellar surface with an angular separation of 55° and not 180° as seen in the case of a centred dipole. Respectively, the two magnetic poles form a large "magnetic spot". High-resolution spectra were obtained allowing He I and Si II abundance variations to be studied as a function of rotational phase. The results show that the helium abundance is concentrated in one hemisphere of the star, near the magnetic poles and it is comparatively weaker in another hemisphere, where magnetic field lines are horizontal with respect to the stellar surface. At the same time, the silicon abundance is greatest between longitudes of $180 - 320^\circ$, the same place where the helium abundance is the weakest. These abundance variations (with rotational phase) support predictions made by the theory of atomic diffusion in the presence of a magnetic field. Simultaneously, these result support the possibility of the formation of unusual structures in stellar magnetic fields. Analysis of vertical stratification of the silicon and helium abundances shows that the boundaries of an abundance jump (in the two step model) are similar for each element; $\tau_{5000} = 0.8-1.2$ for helium and $0.5-1.3$ for silicon. The elemental abundances in the layers of effective formation of selected absorption lines for various phases are also correlated with the excitation energies of low transition levels: abundances are enhanced for higher excitation energy and higher optical depth within the applied model atmosphere.

Key words:

stars:chemically peculiar–
stars:magnetic fields–
stars:atmosphere–
stars:individual: HD 21699

1 INTRODUCTION

HD 21699 (HR 1063) was initially classified by Roman and Morgan (1950) as a B8IIIvar star. Molnar (1972) later performed an analysis of its spectra and determined that helium was extremely deficient (by factor of 5), as a result he classified this star as a He-weak. Shore et al. (1987) refer to HD 21699 as a He-weak silicon star (sn class - with broad and diffuse He I lines). The Sn class is primarily attributed by Morgan (1977) to the silicon and He-weak star HD 5737. In the classification of Preston (1974) both objects

are categorised as chemically peculiar (CP2) stars. Because of the extremely reduced helium abundance, it is possible that HD 21699 has been given an incorrect spectral classification: the MK classification gives Sp = B8, whereas Abt et al. (2002) suggest a spectral class of B8IIIpMn that corresponds to $T_{\text{eff}} = 12000$ K, while Glagolevskij (2002) derived $T_{\text{eff}} = 16100$ K from the analysis of colour indices. Using the spectra obtained with the 6-m telescope, the following parameters were derived by Glagolevskij et al. (2006) by an analysis of the H_δ line: $T_{\text{eff}} = 16000$ K, $\lg g = 4.15$, $V_i = 0.8 \text{ km s}^{-1}$.

The period of axial rotation for HD 21699 is $P = 2^d.4765$ (Brown et al. 1985). Using the relation between the equatorial velocity (km s^{-1}), period (days), stellar radius in solar radii ($V = 50.613 * R/P$) and the measured value of $v \sin i = 35 \text{ km s}^{-1}$ yields an inclination angle of $i = 32^\circ$ (Glagolevskij & Chuntunov 2007). The positive magnetic field maximum occurs at the phase $\phi = 0$, and the negative extremum occurs at $\phi = 0.4$, according to the ephemerides of Glagolevskij & Chuntunov (2007) for initial phase; (JD = 2445595.529 + $2^d.49246$)

2 MAGNETIC FIELD MODEL AND VARIABILITY OF HE I AND SI II LINES

It has been shown by Stateva (1995) that a one-spot model for the helium and silicon surface distributions fits the observed periodic equivalent width variations in both He I lines and Si II lines. In this case one large He-weak spot is situated around the positive magnetic pole, while the Si II spot is located at the negative pole, with the surface magnetic field assumed to be due to a centered dipolar field. Analysis of the equivalent widths of the helium and silicon lines show that the maximum values do not occur at the same phase and are in fact opposite. Usually, in a case of centered magnetic dipole the abundances of the same element are equal in the vicinity of both magnetic poles. UVB photometry (Percy 1985) shows only a single "peak" in the light curve during one complete rotational period; typically stars with a centered dipolar magnetic field display a double wave (one peak and trough). In the work of Shore et al. (1987) it is mentioned that a similar behavior is noted in the photometric data of two other He-weak stars: HD 5737 and HD 79158.

Brown et al. (1985) reported the discovery of magnetically controlled stellar mass outflow in HD 21699 based on IUE observations of the C IV resonance doublet, which is variable on the rotational time-scale of about 2.5 days, but found only one jet from one of the magnetic poles.

An additional study of the surface magnetic field for this star was performed by Glagolevskij & Chuntunov (2007) using a model of the spatially distributed magnetic charges (Gerth & Glagolevskij, 2001). This approach differs from other methods and could be considered more representative of the real physics because the magnetic field should have a vortex current source. Varying the necessary parameters, authors have calculated phase curves of the mean effective field B_e and of the mean surface magnetic field B_s , which have then been compared with observed data. By the method of successive approximation (step-by-step approach) they have found the best fit between the calculated data and the observations.

Measurements of the H_β line with the Zeeman polarimeter (Brown et al. 1985) were employed to constrain the magnetic field model. A better agreement between the observed and calculated equivalent widths curves of He I and Si II lines for HD 21699 is reached with a model where the dipole is displaced across its magnetic axis from the stellar center by a distance $a = 0.4 \pm 0.1$, expressed in stellar radii units. Therefore in this configuration the magnetic poles appear to be close to one another on the stellar surface (they are separated by 55° , not by 180° , as it would be in the case

of a centered dipole). The big "strong" helium spot is situated at the average position of the two magnetic poles, while the "weak" spot is located on the opposite side of the star (Glagolevskij & Chuntunov 2007).

The equivalent widths of He I and Si II lines show extreme values at phases that correspond to the passage through the visible meridian of zero magnetic field between the magnetic poles. The intensity of the helium line reaches its maximum at the magnetic poles, while the intensity of the silicon lines reaches its minimum in the same place. Silicon abundance is maximal in the regions where the magnetic field is predominantly tangential to the stellar surface.

The behavior of atomic diffusion does not depend on the sign of the magnetic field nor does the abundance of chemical species in a magnetic spot depend on the field's sign. Observational data shows that despite the helium lines being weakened in all rotational phases, the helium is clearly enhanced at the magnetic spot and on the contrary, silicon lines are weaker in that spot than on the opposite part of the stellar surface. Due to averaging over the visible hemisphere and owing to the close location of both magnetic poles to each other, the only intensity variation (one wave) in spectral lines is observed for the two investigated chemical species. For the same reason we observe only one wave variability in the photometric light curve and for average surface magnetic field B_s . Respectively, only one stellar wind jet, common from both poles, is observed.

HD 21699 is a unique star when taking into account the nature of the surface magnetic field distribution. Due to the close proximity of the positive and negative magnetic poles to each other, the common "magnetic spot" is situated on the half of the stellar surface with predominantly vertical magnetic field lines (Glagolevskij & Chuntunov, 2007), while in the other hemisphere magnetic field lines are horizontal. Such a magnetic field configuration provides an excellent "lab" for studying abundance surface distributions of chemical species concentrated around magnetic poles (He I and others) and those that are concentrated in areas with horizontal magnetic field lines (Si II and others). It also provides a unique opportunity to study the variability of mean abundances with rotational phase, and the vertical distribution (stratification) of chemical species in stellar atmospheres depending on the structure of the magnetic field.

HD 21699 is a very suitable star for studying the atomic diffusion of chemical species in the atmospheres of CP stars because its surface can be simply divided in two parts: one, where the magnetic field lines are horizontal to the stellar surface, and another, where they are predominantly vertical.

3 OBSERVATION DATA AND TREATMENT

Medium-resolution spectra were obtained using the main stellar spectrograph (MSS) (equipped with a slicer of 14 cuts and spectral resolution $R = 15000$) on the 6-m telescope of the Special Astrophysical Observatory of Russian Academy of Sciences (SAO RAS). Nine spectra in the region 3900-4300 Å were obtained to uniformly cover the whole rotational period, with a signal-to-noise ratio of 2000. One additional higher resolution spectrum was obtained with the Nasmyth Echelle Spectrometer (NES, see Panchuk et al. 2002) for a resolution of 40000 in the range 4500-5900 Å

Table 1. Data of observed spectra (JD, wavelength coverage, S/N and rotational phase)

JD	spectrograph	wavelength cov.	S/N	phase
2453591.6342	MuSiCos	4490 - 6620 Å	300-410	0.118
2453594.6357	"	"	340-450	0.322
2453607.6030	"	"	240-360	0.525
2453605.510	NES	4500 - 5900 Å	300	0.687
2454072.444	MSS	4000 - 4240 Å	2000	0.023
2454070.182	"	"	"	0.116
2454464.188	"	"	"	0.195
2454073.167	"	"	"	0.314
2454462.189	"	"	"	0.393
2454073.558	"	"	"	0.470
2454101.155	"	"	"	0.543
2454485.251	"	"	"	0.646
2454072.208	"	"	"	0.928

(the phase=0.687). The signal-to-noise ratio for this spectrum is 300. The SAO spectra are reduced using MIDAS procedures.

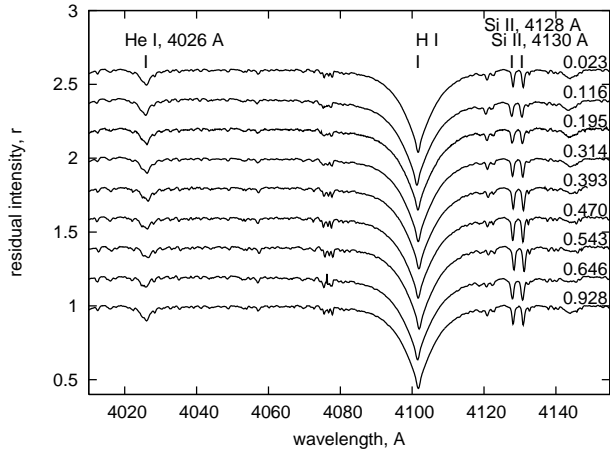
We also used spectropolarimetric data (Stokes I and V) obtained with the MuSiCoS (MUlti SIte COntinuous Spectroscopy) spectropolarimeter which was installed on the 2-m Bernard Lyot telescope at the Pic du Midi Observatory in France. MuSiCoS is a table-top cross-dispersed echelle spectrograph which is fed by two optical fibres from the polarimeter, mounted in the cassegrain focus, with resolution $R = 35000$ and wavelength coverage from 4500 to 6600 Å (phases=0.118, 0.322, 0.525). The signal-to-noise ratio for the MuSiCoS spectra is about 400 per pixel.

A complete Stokes exposure is made up of 4 subexposures in which the retarder is rotated by 90 degrees and back. In principle any first order spurious polarization signatures are suppressed to an acceptable level, by switching the beams within the instrument. The MuSiCoS spectra are reduced using the ESPRIT data reduction package (Donati et al. 1997). We only used Stokes I spectra from the MuSiCoS data, which were obtained with observing procedures described in detail by Donati et al. (1999). Stokes V spectra are not discussed here simply because the three available phases are not sufficient to provide additional information about the magnetic field geometry.

In Table 1 we provide the JD, wavelength coverage, S/N and rotational phase for all spectra. The nine spectra obtained with MSS SAO RAS are shown in Fig.1, where we can see variation in intensity of He I 4026 Å, Si II 4128 Å and 4130 Å lines during rotational period.

4 THE SPECTRA MODELING

Synthetic spectra for HD 21699 were calculated with the code SYNTHM of Khan (2004) and SYNTHV of Tsybal (1996), both codes calculate the line profiles or synthetic spectra formed from the entire visible hemisphere of the star. We used Kurucz's model atmospheres (1994) as well

**Figure 1.** Nine spectra of HD 21699 obtained with MSS SAO RAS. We can see variation of intensity of He I 4026 Å, Si II 4128 Å and 4130 Å lines during rotational period.

as Pavlenko's (2003) model atmospheres with a reduced He abundance. The atomic lists of VALD (Kupka et al.1999) and Castelli (<http://wwwuser.oat.ts.astro.it/castelli/>) were used as the input atomic data for the spectrum synthesis. The average abundance of each chemical species (assuming no vertical stratification) was determined by comparing observed spectral profiles to those produced by the models: SYNTHV code (no magnetic splitting) and SYNTHM code, that takes into account magnetic splitting of lines (Version-04 without stratification). Stratification of chemical elements was determined in a similar vein using the SYNTHM code (Version-05). Previously, we have determined the contribution function for each line using the code WITA (Pavlenko 1997).

5 RESULTS

HELIUM: The helium lines are weakened in the spectra of HD 21699. Osmer and Peterson (1974) and Vauclair (1975) have shown that the formation of He-weak or He-rich stars depends on the wind power in their atmospheres. If we define VW as the relative velocity of flux with respect to a stellar wind and VD as the velocity of diffusion inside a star, then He-weak stars are formed when $VD > VW$ (Vauclair 1975). It is clear from Fig. 2 that over the whole surface of HD 21699, helium appears to be deficient. Nevertheless, in the area of the "magnetic spot" the helium abundance is comparatively higher (by a factor 1.5), than what is derived for the opposite side.

In Fig. 2 we show the variation of helium abundance with the rotational phase. Circles represent the averaged abundance obtained from analysis of four He I lines (4026 Å in SAO MSS spectra and 4713, 4921, 5015 Å in the MuSiCoS spectra), while the squares represent an abundance deduced only from one He I line (4026 Å) using SAO MSS spectra). Errors in the averaged He abundances, estimated from the standard deviation of the data obtained for all analyzed He lines at respective rotational phases, are specified by vertical bars. The uncertainty for the single He I 4026 Å abundances for all phases was estimated as 0.1 dex. All the

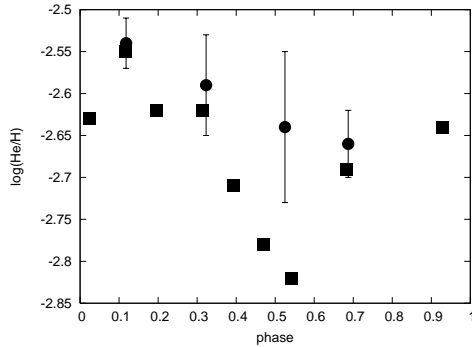


Figure 2. Variability of the helium abundance ($\log N(\text{He})/N(\text{H})$) with rotational phase. The circles indicate abundances deduced from analysis of four He I lines (MuSiCoS and NES spectra), while the squares indicate abundances deduced from analysis of the He I line 4026 Å. All abundance values are averaged over the visible hemisphere for each phase (see Table.1), not taking into account helium stratification in the atmosphere and presence of spots.

results for Fig. 2 were obtained using SYNTHM code which takes into account magnetic splitting of spectral lines. The abundance estimates are derived for the visible hemisphere for each phase.

For those parts of the stellar surface where the magnetic lines are horizontal, only vertical diffusion of He I (not He II) is efficient. The helium abundance in the aforementioned parts of stellar surface must be higher than at the magnetic poles, where the field lines are vertical, because there is no resistance to diffusion by both the He I and He II atoms. The fact that the intensity of He I lines at the magnetic poles is higher than on the opposite side supports the idea of a sufficiently strong wind at the magnetic poles. The observed data justify the presence of a powerful wind from the "magnetic spot" of HD 21699 (magnetically structured jets, Brown et al. 1985). We have assumed the two-step approximation for vertical stratification of chemical species in the atmosphere of HD 21699 (see, for example, Ryabchikova et al. 2005).

For the lower layers, the abundance was derived from the line wings, while for the upper layers it was derived from the line cores. An example of the fit for the He I 4026 Å line profile at phase 0.116 (MSS spectrum) is shown in Fig. 3. It is obvious that the line wings are quite sensitive to the helium abundances at the lower atmospheric layers. Therefore, the respective helium abundance can be specified with high confidence, namely with an error of 0.1 dex. Meanwhile, the core of a line provides information about the element abundance in the upper atmospheric layers. However, it provides a somewhat larger error, 0.2 dex. Only by taking into account the He stratification we can get a good fit between the model and the observed diffuse He line profiles for this He-weak sn-type star.

In Fig. 4 we show the vertical stratification of helium for nine phases, derived from the analysis of the He I 4026 Å line profiles using the Kurucz model atmosphere 16000/4.0 for the visible hemisphere for each phase.

The results shown in Fig. 4 confirm the theoretical prediction of Vauclair et al. (1991), which predict the enhancement of helium abundance towards a deeper optical depth. In Fig. 5, we can see that as the phase changes, the opti-

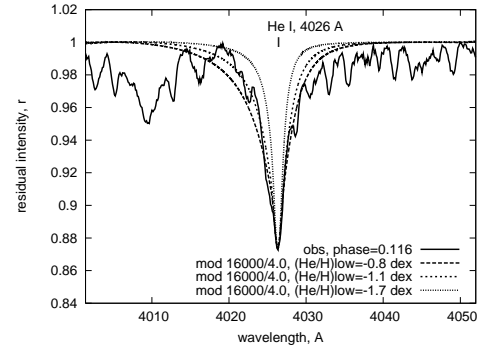


Figure 3. The fits of calculated He I 4026 Å line profiles to observed one for phase 0.116. Here $(\text{He}/\text{H})_{\text{low}}$ specifies helium abundance at the lower atmospheric layers assuming the two steps model for helium vertical stratification.

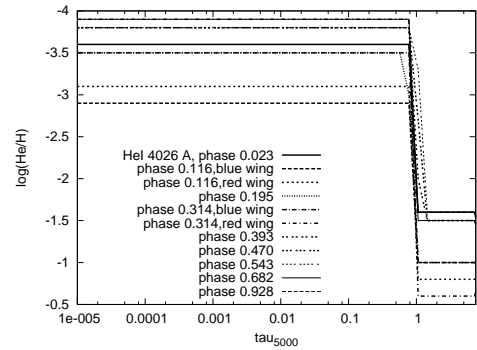


Figure 4. Helium vertical stratification (in the frame of two-step model) from the analysis of He I 4026 Å line for various rotational phases. In phases 0.928, 0.023, 0.116, 0.195, 0.314 helium abundance is close to its maximum, while in phases 0.393, 0.470, 0.543, 0.682 helium abundance is close to its minimum.

cal depth τ_{5000} corresponds to where the abundance jump behaves inversely to the variation of the He abundance (see Fig.2).

SILICON: In Table 2, we show estimates of the silicon abundance derived from MuSiCoS and NES spectra for seven Si II lines with various excitation energies (in the range of 8-16 eV) of the lower transition level for 4 rotation phases. These values were obtained for the visible hemisphere for each phase without taking into account the silicon strati-

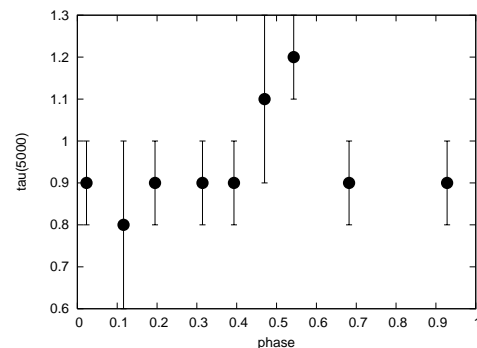


Figure 5. Optical depth τ_{5000} of the abundance jump with bars of errors versus rotational phase for the line He I 4026 Å .

Table 2. Variation of Si II mean abundance for 4 rotational phases: 0.118, 0.322, 0.525 are from MuSiCoS spectra and 0.687 is from NES spectrum.

line (Å)	EP(eV)	log N(SiII)/N(H) vs. phase			
		0.118	0.322	0.525	0.687
6347	8.12	-5.12	-4.92	-4.02	-
6371	8.12	-5.12	-4.92	-4.12	-
5041	10.07	-4.87	-4.67	-4.02	-4.25
5055	10.07	-5.15	-4.99	-4.55	-4.50
4673	12.84	-3.87	-3.82	-3.52	-3.70
5669	14.21	-4.15	-4.05	-3.55	-3.75
5202	16.35	-3.75	-3.80	-3.20	-3.70

Table 3. Variation of mean silicon abundance log N(SiII)/N(H) (without stratification) with rotational phase (including MSS spectra): the phases 0.118, 0.322 and 0.525 Å are taken from MuSiCoS spectra, the phase 0.687 is NES spectrum. Wavelengths and EP of spectral lines are given in Table 2.

Phase	mean 4128,	mean (MuSiCoS & NES)		
	4130Å, EP=9.84	8-10eV	12-16eV	Si III 4552Å
0.023	-4.90			
0.116	-4.95			
0.118	-	-5.06	-3.92	-3.77
0.195	-5.15			
0.314	-4.80			
0.322	-	-4.88	-3.89	-3.75
0.393	-4.50			
0.470	-4.35			
0.525	-	-4.16	-3.42	-3.77
0.543	-4.35			
0.682	-4.15			
0.687	-	-4.37	-3.72	
0.928	-4.70			

fication in the atmosphere of the star. It is easy to track an apparent increase of the derived silicon abundance with the rise of excitation energy (i.e., towards the deeper atmosphere). This tendency supports the idea of vertical stratification of silicon as suggested by Vauclair et al. (1979).

Table 3 shows a combination of the aforementioned data with the silicon abundances derived from Si II lines 4128 Å and 4130 Å for nine rotational phases using the MSS spectra. Fig. 6 presents them graphically as a variation of silicon (Si II) abundance with rotational phase. These abundance estimates, like He I abundances for all phases, were obtained with the SYNTHM code taking into account magnetic splitting for values B_s corresponding to each phase from the magnetic field model. We see that silicon has a higher abundance where the surface magnetic field has the lowest value (phases 0.525, 0.543, 0.682).

Taking into account the level (-4.49 dex) of solar abundance for silicon (Grevesse et al. 2007), it appears that the lines with low excitation energies show an abundance deficit,

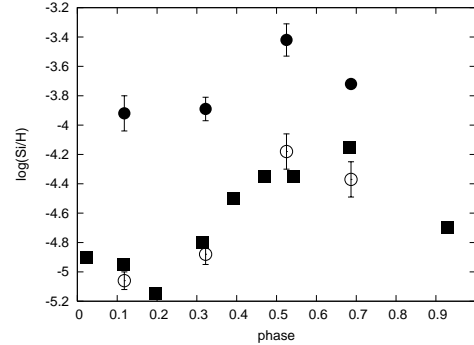


Figure 6. Variation of silicon (Si II) abundance with rotational phase. The estimates of log N(Si)/N(H) are derived from the lines of low excitation energies (clear circles stand for eshelle, MuSiCoS and NES spectra, while shaded squares stand for MSS spectra) and high excitation energies (shaded circles stand for eshelle spectra). Vertical bars show errors of the averaged estimates. The error for single abundances was estimated as 0.1 dex

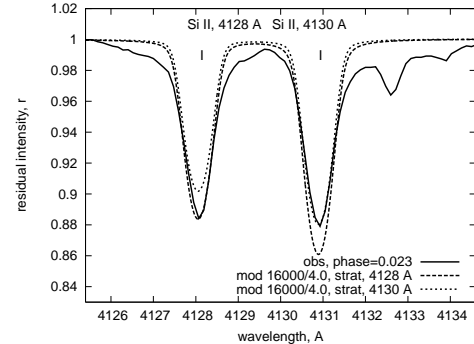


Figure 7. The fit of Si II lines 4128 and 4130 Å to model profiles, calculated taking into account magnetic broadening and stratification of silicon in the atmosphere.

while the lines with high excitation energy show an excess of silicon for the phases with maximal B_s (0.118 and 0.322).

We also determined Si III abundance from the 4552 Å line using the same model atmosphere 16000/4.0 (see last column of Table 3) for the three phases of MuSiCoS spectra. The results are close to abundances derived from the Si II lines of high excitation energies, justifying the choice of the model atmosphere.

It is remarkable that the abundance estimates derived from the analysis of lines with low excitation energies are in good agreement among themselves for all available spectra (MuSiCoS, NES and MSS). For the phases with minimal B_s (0.525 and 0.687) all the lines show an excess of silicon. Nevertheless, the lines with higher excitation energies still result in higher silicon abundance. They formed at deeper atmospheric layers and as a result we observe an enhancement of silicon abundance there. This is most obvious in the case of the "magnetic spot". In Fig.7 we show the fit of Si II lines 4128 and 4130 Å to model profiles, calculated by taking into account magnetic broadening and stratification of silicon in the atmosphere. Note the relatively good fits of profiles.

Fig. 8 shows an enhancement of silicon abundance towards the deeper atmospheric layers, as predicted by Vauclair et al. (1979). Fig. 9 presents stratification of Si II de-

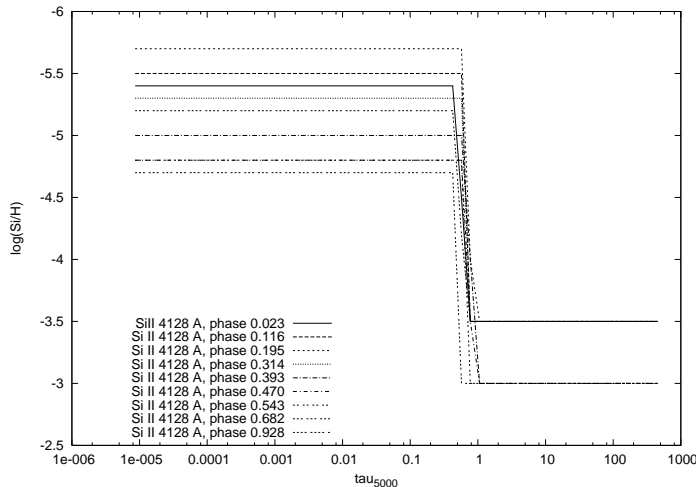


Figure 8. Vertical stratification of silicon deduced from analysis of Si II line 4128 Å assuming the two-steps model. Phases 0.023, 0.116, 0.195, 0.314, 0.928 correspond to minimal Si II abundance (maximal He I), while phases 0.393, 0.410, 0.470, 0.543, 0.682 correspond to maximal Si II abundance (minimal He I).

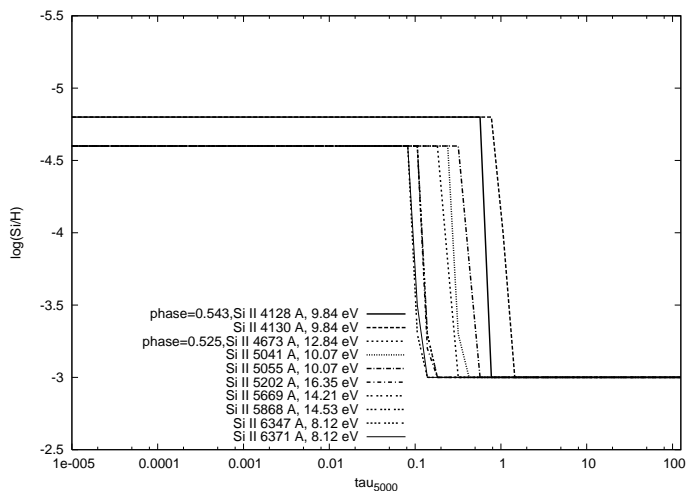


Figure 9. Vertical stratification of silicon for the phase 0.525, where B_s reaches its minimum and Si II abundance rises to its maximum.

rived from lines with different excitation energies for the phase of minimal magnetic field.

The case of non-uniform silicon distribution on the surface of magnetic stars is discussed in the works of Vauclair et al. (1979), Alecian and Vauclair (1981) and Megessier (1984). Silicon usually accumulates in the places where the magnetic field lines are predominantly horizontal and where they can oppose the gravitational settling of ionized silicon. In the case of a shifted magnetic dipole, like HD 21699, the side opposite to the magnetic poles has a large area with horizontal magnetic field lines, where silicon should be concentrated. Meanwhile, it has to be weakened around the magnetic poles.

From Tables 2 and 3 and Fig. 6, 7 and 8 it appears that our results confirm the predictions of Vauclair et al. (1979), Alecian and Vauclair (1981) and Megessier (1984). In the atmosphere of HD 21699 silicon is enhanced in the area

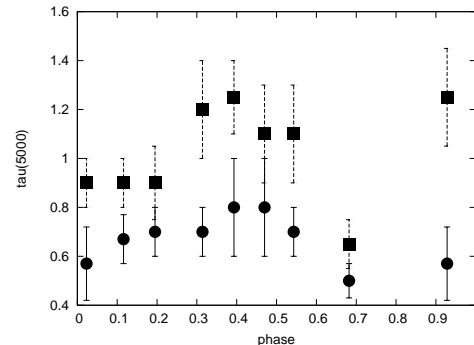


Figure 10. Optical depth τ_{5000} of the abundance jump versus rotational phase for the Si II lines 4128 Å (filled squares) and 4130 Å (filled circles) with bars of error. As in the case of He I, we can see a tendency to change τ_{5000} with phase contrary to abundances.

where the field lines are horizontal to the stellar surface. The optical depth of the abundance jump for silicon τ_{5000} (like to helium) has a tendency to change with phases reversely to the silicon abundance variation (see Figs. 6, 10).

Abundance stratification due to diffusion processes acting in the atmospheres of chemically peculiar stars is studied in the recent work of Monin & LeBlanc (2007). Their self-consistent models show that elements such as Fe, Cr, Si and Ca do indeed accumulate at large optical depths, while they are dramatically underabundant in the upper atmosphere. The transition zone for iron in their models is located around optical depth $\tau_{5000} = 1$.

6 BASIC CONCLUSIONS

For the first time photospheric chemical element abundances of HD 21699 were obtained during the whole rotational period. Magnetic splitting of spectral lines and elements stratification in the atmosphere were taken into account with line profile modelling. Helium abundance is weakened for the whole stellar surface, which is usual for He-weak stars. Nevertheless, helium has higher abundance in the region of the "magnetic spot" due to the influence of stellar wind, which elevates the helium to the outer layers of the stellar atmosphere, and helium abundance should increase with optical depth in the atmospheres of He-weak stars. (Vauclair et al. 1991).

Silicon is accumulated in the part of the star where the magnetic field lines are predominantly horizontal, as it was predicted by Vauclair et al. (1979), Alecian and Vauclair (1981) and Megessier (1984). Silicon abundance determined from lines with low excitation energies (8-10eV) appears to be lower in the area of the magnetic poles and is approximately solar in the region with horizontal magnetic lines. The lines with high excitation energies (12-16eV) also show enhancement of silicon abundance for the region with horizontal magnetic lines, but this abundance is significantly higher than solar everywhere on the stellar surface. Silicon abundance is lower in the outer parts of the atmosphere and higher in the deeper layers.

The optical depth of the abundance jump (in two-steps model) is near to $\tau_{5000} = 1$. In the cases of He I and Si II, we

can see a tendency to change τ_{5000} with the phase contrary to abundances, which could be the result of competition between the stellar wind, diffusion, and the local magnetic field geometry that would lead to accumulations of helium and silicon at different depths in the atmosphere.

Since IUE observations of the C IV resonance doublet show existence of magnetically controlled stellar wind in HD 21699 (Brown et al. 1985), one should expect some variations in Balmer lines, similar to that seen in H-alpha in 36 Lyn (Wade et al. 2006) and in HD 37479 (Smith et al. 2006) and in many Balmer lines in HD 37479 (Smith and Bohlender, 2007). Unfortunately, due to the incomplete number of observed phases it is difficult to find similar changes in Balmer lines in HD 21699.

7 ACKNOWLEDGEMENTS

We thank V. Tsymbal and S. Khan for the use of their codes: SYNTHV and SYNTHM. Many thanks to the referee of the paper, Dr. Bohlender for the very valuable advice and comments. This work was partially funded by the Microcosmophysics program of National Academy of Sciences and National Space Agency of Ukraine and by the Natural Sciences and Engineering Research Council of Canada (NSERC).

REFERENCES

- Abt H.A., Levato H., Grosso M., 2002, ApJ, **573**, 359
 Alecian G. and Vauclair S., 1981, A&A, **101**, 16
 Brown D.N., Shore S.N., Sonneborn G., 1985, Astron.J., **90**, 1354
 Castelli F., <http://wwwuser.oat.ts.astro.it/castelli/linelists.html>
 Donati J.-F., Semel M., Carter B.D., Rees D.E., Cameron A.C., 1997, MNRAS, **291**, 658
 Donati J.-F., Catala C., Wade G.A., Gallou G., Delaigüe G., Rabou P., 1999, A&AS, **134**, 149
 Gerth E., Glagolevskij Yu. V., 2001 in Magnetic Fields Across the Hertzsprung-Russell Diagram, ASP Conference Proceedings, Edited by G. Mathys, S. K. Solanki, and D. T. Wickramasinghe, **248**, 333
 Glagolevskij Yu. V., 2002, Bulletin of the Special Astrophysical Observatory, **53**, p. 33
 Glagolevskij Yu.V., Leushin V.V., Chuntunov G.A., Shulyak D., 2006, Astronomy Letters, **32**, 54
 Glagolevskij Yu.V., Chuntunov G.A., 2007, Astrophysics, **50**, 362
 Grevesse N., Asplund M., Sauval A., 2007, J.Space Science Reviews, **130**, Issue 1-4, pp. 105
 Khan S., 2004, J. Quant. Spectrosc. Radiat. Transfer., **88**, 71
 Kurucz R.L., 1993-1994, Kurucz CD-ROM No. 1-22, Cambridge, Mass.: Smithson. Astrophys. Obs.
 Kupka F., Piskunov N., Ryabchikova T.A., Stempels, H. C., Weiss, W. W., 1999, A&AS, **138**, 119
 Megessier C., 1984, A&A, **138**, 267
 Molnar M.R., 1972, ApJ, **175**, 454
 Monin D., Leblanc F., 2007, in Physics of Magnetic Stars, Eds. I.I.Romanyuk and D.O.Kudryavtsev, SAO RAS, Nizhnij Arkhys, Russia, p.360
 Morgan W.W., 1977, Bulletin of the American Astronomical Society, **9**, 293
 Osmer P.S., Peterson D.M., 1974, ApJ, **187**, 117
 Panchuk V., Piskunov N., Klochkova V., Yushkin V., Ermakov S., 2002, Preprint SAO RAS, **169** (in Russian)
 Pavlenko Ya.V., 1997, Ap&SS **253**, 43
 Pavlenko Ya.V., 2003, Astron. Rept. **47**, 59
 Percy J.R., PASP, 1985, **97**, 856
 Preston G.V., 1974, Ann.Rev.A&A, **12**, p.257
 Roman N.G., Morgan W.W., 1950, ApJ, **111**, 426
 Ryabchikova T., Leone F, Kochukhov O., 2005, A&A, **438**, 973
 Shore S.N., Brown D.N., Sonneborn G., 1987, Astron.J., **94**, 737
 Stateva I.K., Astrophys. Sp. Sci., 1995, **226**, 329
 Tsymbal V., 1996, in: Model Atmospheres and Spectrum Synthesis, eds. S. J. Adelman, F. Kupka, and W. W. Weiss, ASP Conference Series **108**, 198
 Vauclair S., 1975, A&A, **45**, 233
 Vauclair S., Hardorp J., Pederson D.M., 1979, ApJ, **227**, 526
 Vauclair S., Dolez N., Gough D.O., 1991, A&A, **252**, 618
 Wade G.A., Smith M.A., Bohlender D.A., Ryabchikova T. A., Bolton C. T.; Lueftinger T.; Landstreet J. D.; Petit P. et al., 2006, A&A, **458**, 569
 Smith M.A., Wade G.A., Bohlender D.A., Bolton C.T., 2006, A&A, **458**, 581
 Smith M.A., Bohlender D.A., 2007, A&A, **475**, 1027